

Supporting Information

In-situ Synthesis and Macroscale Alignment of CsPbBr₃ Perovskite Nanorods in Polymer Matrix

Juan He,^{†,‡} Andrew Towers,^{‡,§,‡} Yanan Wang,^{‡,‡} Peisen Yuan,^{||} Zhang Jiang,[∇] Jiangshan Chen,^{||} Andre J. Gesquiere,^{*,†,‡,§,○} Shin-Tson Wu,^{*,†} and Yajie Dong,^{*,†,‡,○}

[†]College of Optics and Photonics, University of Central Florida, Orlando, Florida, USA

[‡]NanoScience Technology Center, University of Central Florida, Orlando, Florida, USA

[§]Department of Chemistry, University of Central Florida, Orlando, Florida, USA

^{||}Institute of Polymer Optoelectronic Materials and Devices, State Key Laboratory of Luminescent Materials and Devices, South China Technology of University, Guangzhou, China

[∇]X-ray Science Division, Advanced Photon Source, Argonne National Laboratory, Argonne, Illinois, USA

[○]Department of Materials Science & Engineering, University of Central Florida, Orlando, Florida, USA

Corresponding Authors:

*andre@ucf.edu

*swu@creol.ucf.edu

*yajie.dong@ucf.edu

[‡]J.H., A.T. and Y.W. contributed equally to this work.

Experimental

Materials:

Polystyrene (PS) substrates were purchased from VWR International, Inc, and polycarbonate (PC) films, acrylonitrile–butadiene–styrene (ABS) films were purchased from McMaster-Carr. CsBr (99.999%), PbBr₂ (99.999%) and N,N-dimethylformamide (extra dry, 99%) were purchased from Sigma-Aldrich. All substrates and materials were used as received.

Synthesis of CsPbBr₃ NRs-PM:

Perovskite precursors CsBr and PbBr₂ were mixed at stoichiometric 1:1 molar ratio and dissolved in dimethylformamide (DMF) solvent with overall concentration of 30mg/ml and stirred at room temperature overnight, and then diluted in DMF to different concentrations of 12, 15, 20 mg/ml. The precursor solution was processed on polymer (e.g. PS) substrates by spin coating at 1000, 2000, 3000 rpm inside a N₂ filled glovebox. The samples were subsequently annealed at 25°C/8h, 40°C/4h or 60°C/2h on a hotplate with no observable brightness/rod morphology difference among different annealing conditions.

Characterization:

Fluorescence microscopy images were taken using an Olympus BX51 microscope. Light source of 450–480 nm was used for excitation.

Synchrotron XRD measurements were carried out at beamline 8-ID-E of the Advanced Photon Source (APS), Argonne National Laboratory. The incident X-ray energy was 10.86 KeV. The sample was mounted in a vacuum chamber in order to reduce air scattering background. A Pilatus 1M area detector (Dectrics Ltd.) mounted 140 mm downstream of the sample was used to collect data. The 2D XRD patterns were converted into 1D plots for further analysis after necessary corrections including detection efficiency and flat field, solid angle, polarization, etc. For convenient comparison, the data present in the manuscript has been converted to 2θ for 8.04 keV which is the energy for commonly used copper K-alpha X-ray.

The PLQY of the films was measured by the integrating sphere method. An intensity-modulated 409 nm laser beam was used for excitation. All the PLQY measurements were carried out in air at room temperature. UV–vis absorption spectra were recorded on a Varian Cary 500 Spectrophotometer at room temperature. The steady-state PL was measured using Ocean Optics USB2000 spectrometer.

A home-built sample-scanning confocal microscope described elsewhere¹ was used for sample radiative lifetime and PL polarization imaging studies. Time correlated single photon counting (TCSPC) excited state lifetime studies were completed by parking an area of interest of the samples over the focused pulsed laser beam (Picoquant LDH-P-C-470), and collecting photons with a fast single photon counting detector (Picoquant, Micro Photon Devices, PDM series). Photon timing was measured using a pulsed laser driver (PDL 800-D) that provided the timing signal to a PicoHarp 300 TCSPC module in combination with a detector router (PHR 800), all from Picoquant. The time-resolved PL decay curves were fitted with a biexponential function of time and the average recombination lifetime is estimated by averaging both time constants with their weighting factors. For PL polarization imaging, circular polarized light generated from the same laser by use of a linear polarizer and a quarter-wave plate was used as the excitation source. The laser was focused to the NRs underneath top surface (spot size of ~300 nm) and the sample was raster scanned across the focused laser beam with a step size of 0.15 μm using a Mad City Labs piezoelectric stage (Nano-LP100) to collect PL images. The light emitted by the sample was split by a broadband polarized beam splitter (BPBS) into two perpendicularly polarized beams that were simultaneously collected by two avalanche photodiodes (PerkinElmer SPCM-AQR-14).

For temperature-dependent PL measurements, the samples were put inside the Linkam LTS350 cryostat, with a heating rate of 5 °C/min. The temperature tunable range was up to 350 °C. Laser excitation at 450 nm (Thorlabs CPS450) was used and the CsPbBr₃ NRs-PM film was in situ heated on the stage whose temperature was controlled by a temperature controller (Linkam TMS 94). The composite films were heated up to a certain temperature, held for 2–3 min to be stable, measured for the spectra (Ocean Optics Spectrometer USB 2000+) and then proceeded to the next temperature point immediately.

Calculation of 1D nanostructure polarization

Because of the cylindrical shape, the electric field polarized parallel to the long axis is not reduced while the electric field perpendicular to the long axis is attenuated and the ratio between the two is²:

$$\frac{E_{\perp}}{E_{\parallel}} = \frac{2\varepsilon_0}{\varepsilon + \varepsilon_0}$$

where ε or ε_0 is the dielectric constant of the cylinder material or the environment material respectively. The dielectric constant of polystyrene is around 2.6, while that of CsPbBr₃ is estimated³ to be 6.35, both in green wavelength range. The ratio between the electric fields of two polarizations is calculated to be ~0.6, and as a result the polarization level P of light intensity is ~0.47.

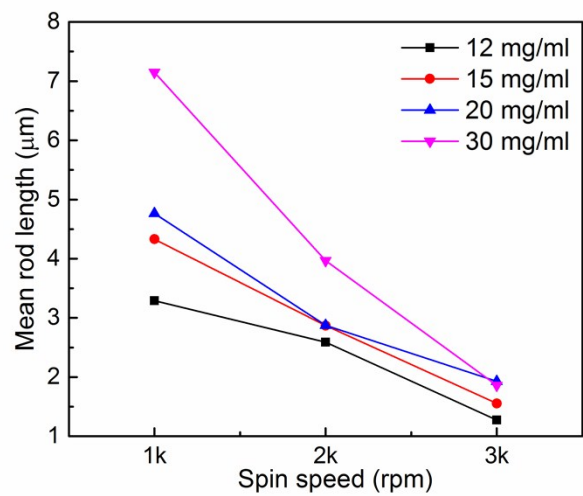


Figure S1. Mean rod length in the CsPbBr₃ NRs-PS synthesized with different precursor solution concentrations and different spincoating speed.

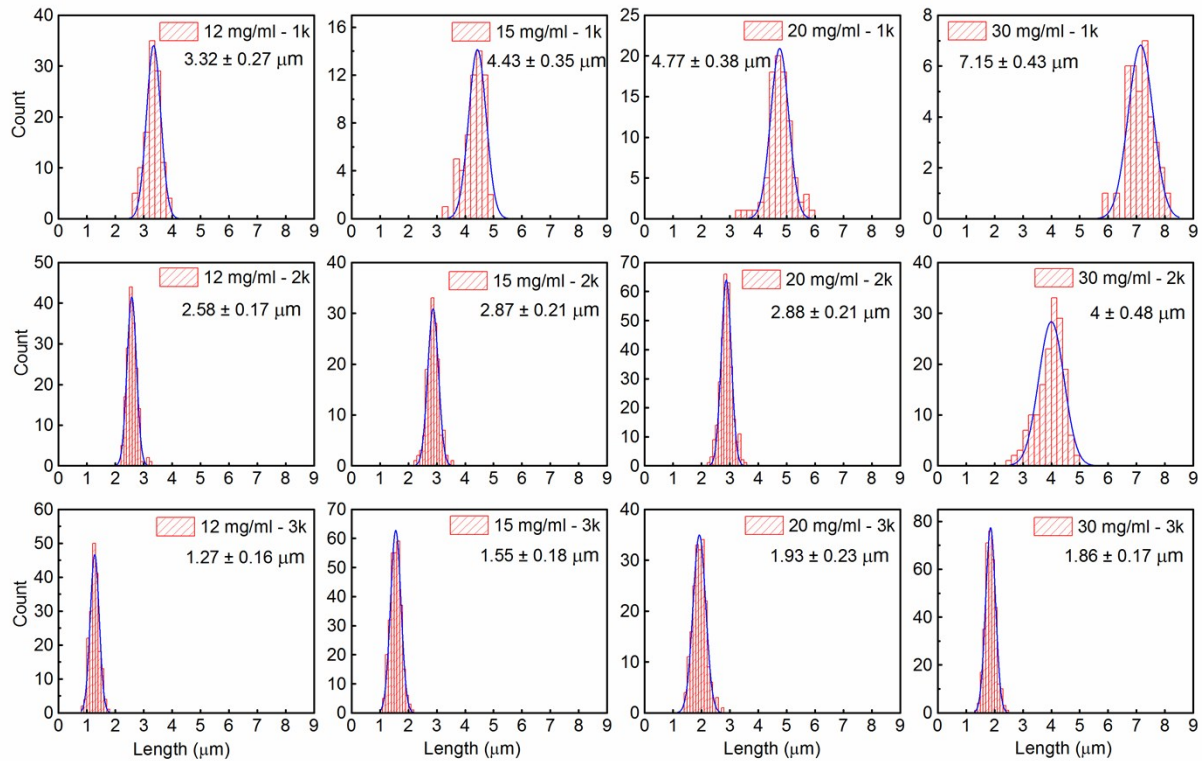


Figure S2. Statistical analysis on rod length distribution in the CsPbBr₃ NRs-PS synthesized with different precursor solution concentrations and different spincoating speed based on fluorescent microscopic images. The distribution was fit to Gaussian (blue) with mean value and standard deviation shown in each diagram.

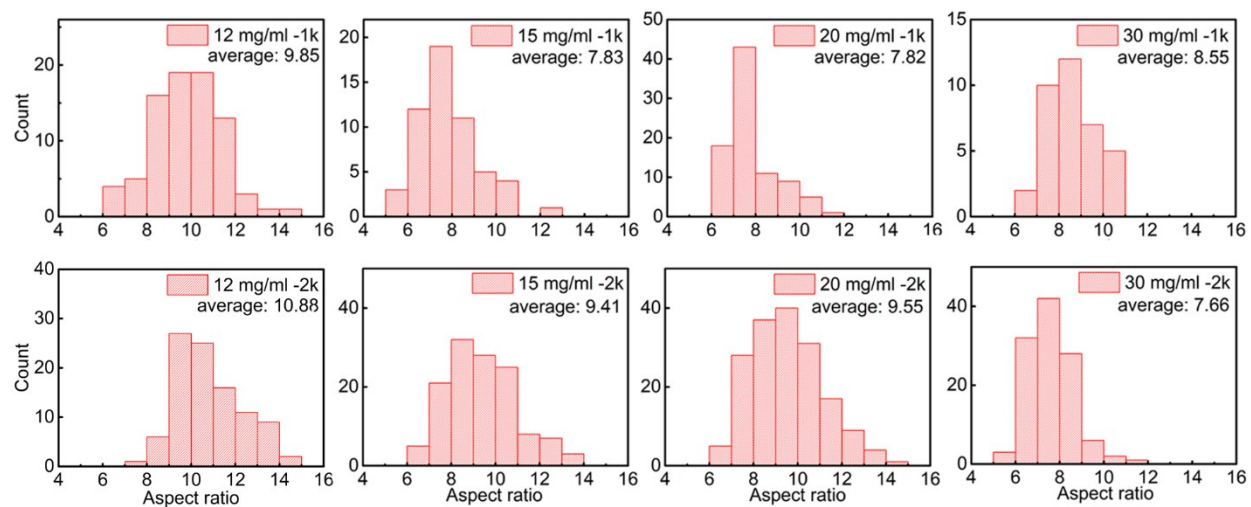


Figure S3. Statistical analysis on aspect ratios of the CsPbBr₃ NRs-PS synthesized at 1000 rpm /2000 rpm spin speed with different precursor concentrations, derived from the fluorescence microscopic images in Figure 1. For the NRs-PS samples prepared at higher spin speed, it is difficult to quantify the width or aspect ratios of the NRs because of the limited resolution of optical microscope images.

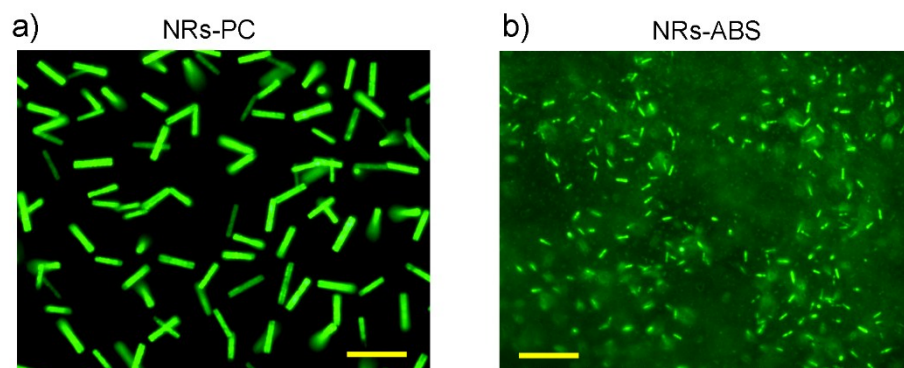


Figure S4. Fluorescent microscopic images of the CsPbBr₃ NRs-PM samples synthesized with different substrates: (a) NRs-PC; (b) NRs-ABS. Scale bar: 10 μ m. Precursor concentration was 30 mg/ml and spincoating speed was 1000 rpm for both.

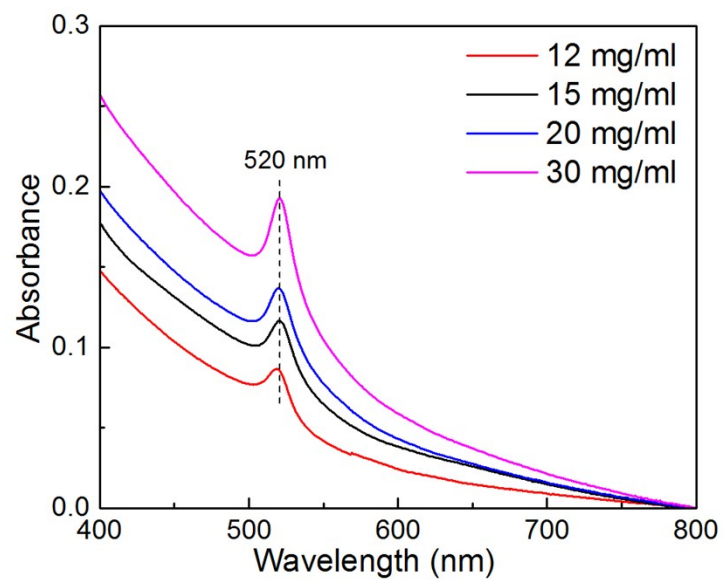


Figure S5. UV-Vis absorption of NRs-PS synthesized with different precursor concentrations.

Table S1. PL spectra peak wavelengths of NRs-PS synthesized with different precursor concentrations and different spincoating speeds.

Spin speed	PL peak wavelength (nm)			
	12 mg/mL	15 mg/mL	20 mg/mL	30 mg/mL
1k	526	526	527	524
2k	524	527	527	527
3k	525	527	527	527

Table S2. Photoluminescence quantum yield (PLQY) of CsPbBr₃ NRs-PS films obtained with different precursor concentrations and different spin-coating speed.

Speed	12 mg/ml	15 mg/ml	20 mg/ml	30 mg/ml
1K	28%	25%	24%	23%
2K	30%	27%	29%	25%
3K	26%	28%	29%	24%

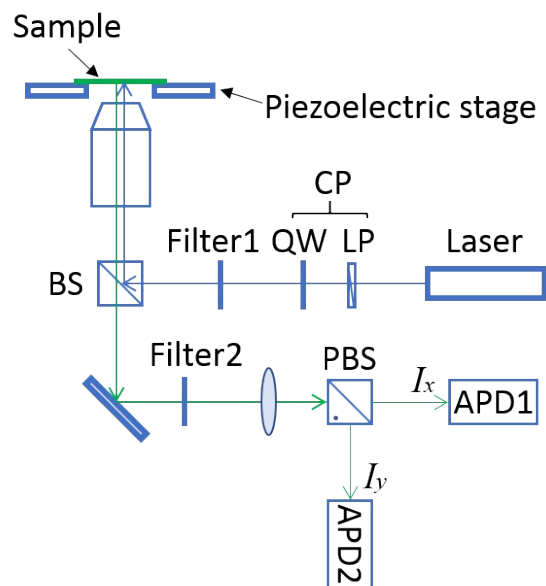


Figure S6. Optical measurement setup of single particle polarization PL imaging. CP: circular polarizer; LP: linear polarizer; QW: quarter-wave plate; BS: beam splitter; PBS: polarizing beam splitter; APD: avalanche photodiode.

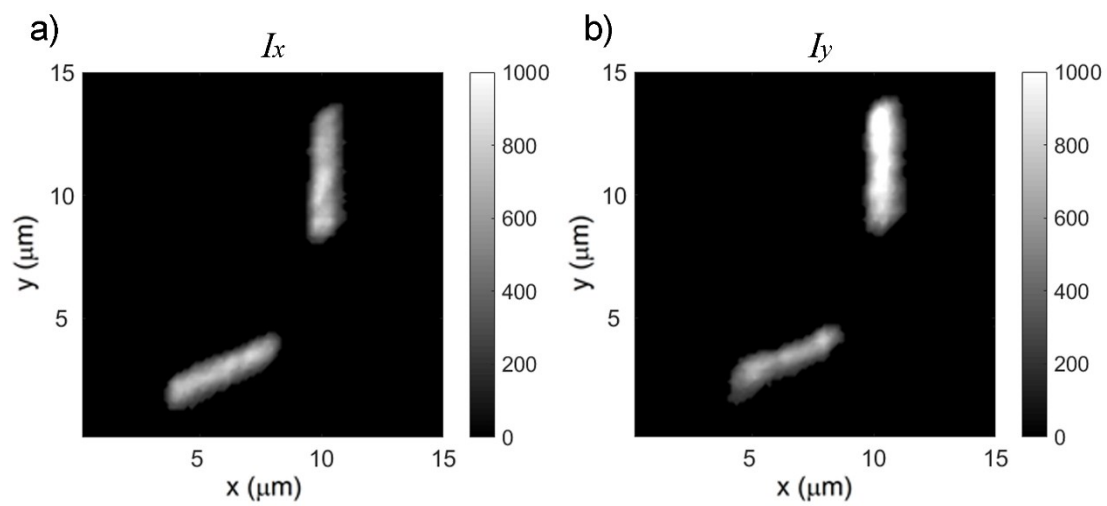


Figure S7. PL images of (a) x and (b) y polarization of the CsPbBr₃ NRs-PS in a local 15 × 15 μm² area.

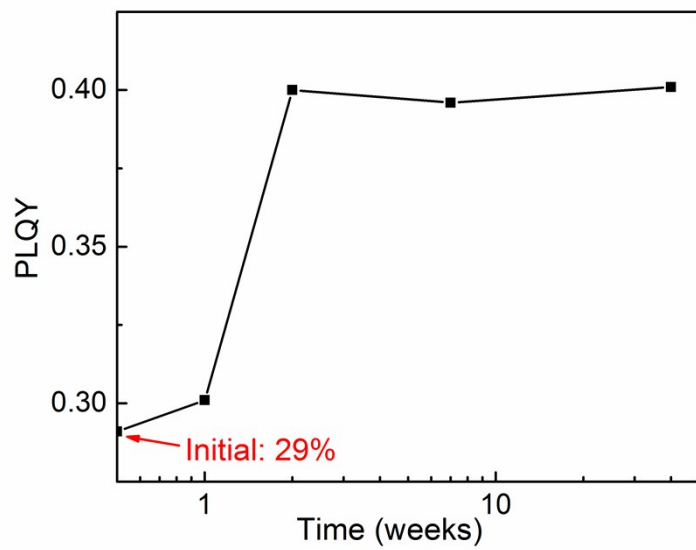


Figure S8. PLQY of CsPbBr₃ NRs-PS film immersed in deionized water at different time.

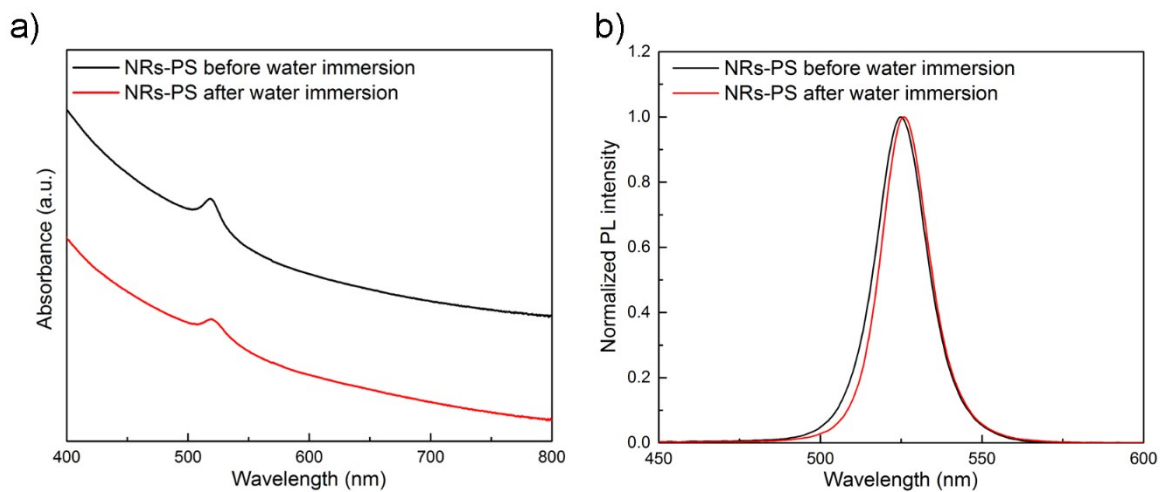


Figure S9. (a) UV-Vis spectra and (b) PL spectra of the CsPbBr₃ NRs-PS film before and after immersion in water for 277 days.

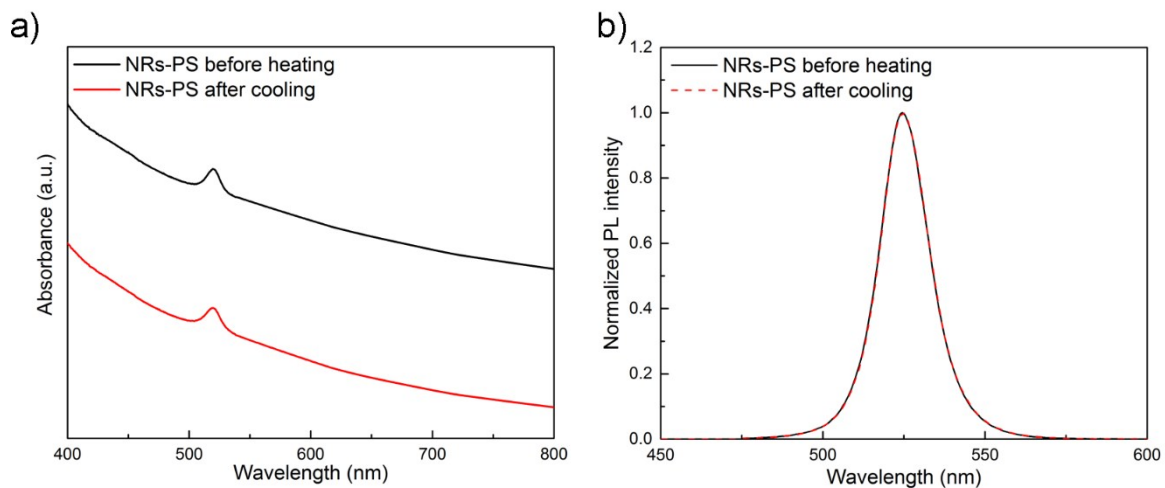


Figure S10. (a) UV-Vis spectra and (b) PL spectra of the CsPbBr₃ NRs-PS film before and after thermal stability measurement.

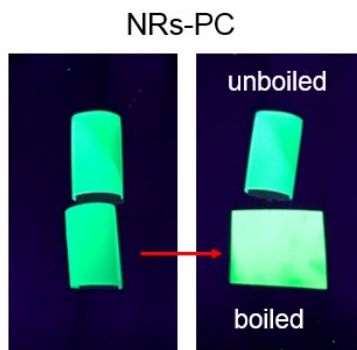


Figure S11. Photographs of CsPbBr₃ NRs-PC film before (left) and after (right) water boiling treatment (lower piece). The upper piece is not boiled for comparison (cutting from one sample). Water enhanced PL is observed for the boiled sample.

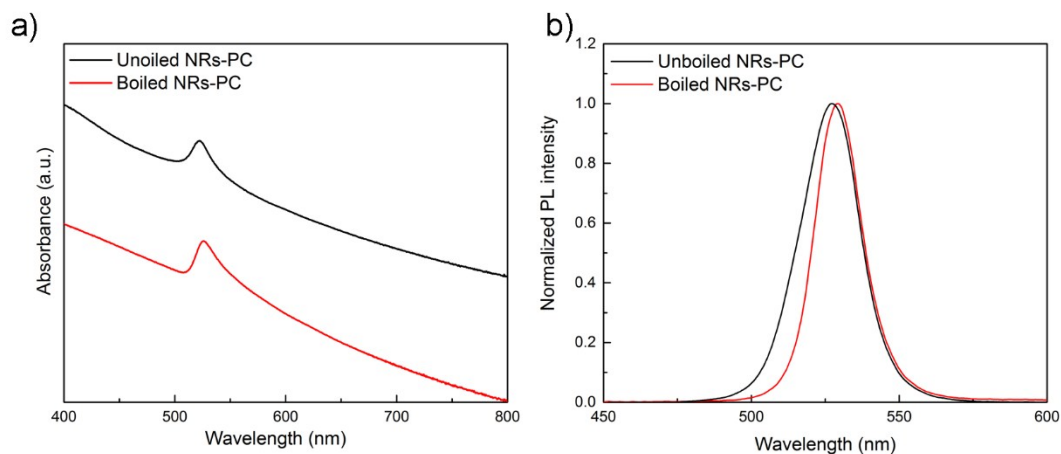


Figure S12. (a) UV-Vis spectra and (b) PL spectra of the CsPbBr₃ NRs-PC film before and after boiling treatment.

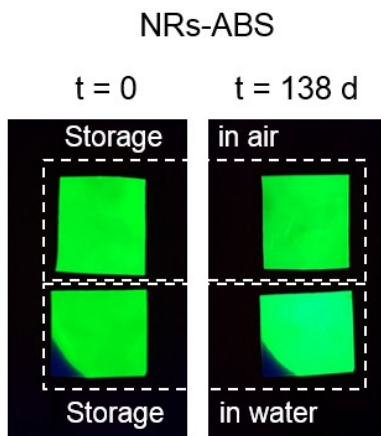


Figure S13. Photographs of CsPbBr₃ NRs-ABS film at the beginning (left) and after 138 days (right) under UV illumination. The upper piece was stored in air and the lower piece was stored in water (cutting from one sample). Water enhanced PL is observed for the sample stored in water.

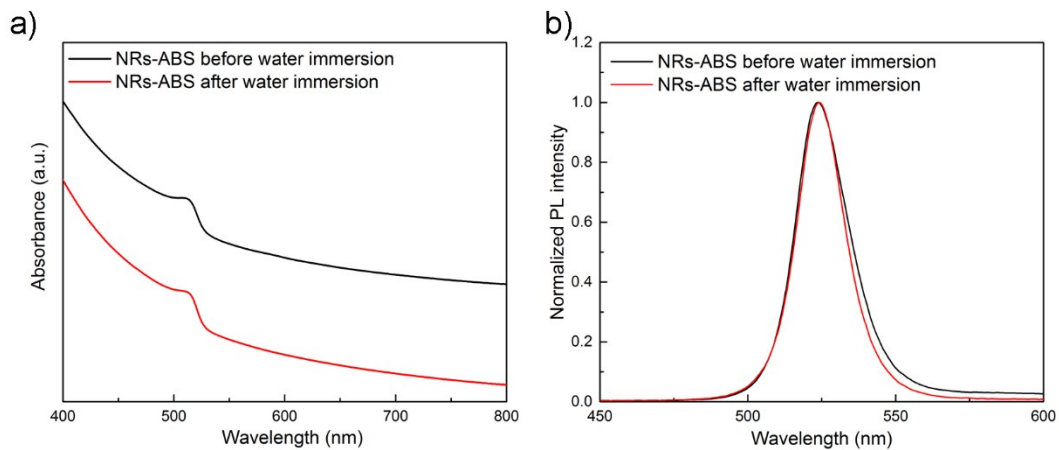


Figure S14. (a) UV-Vis spectra and (b) PL spectra of the CsPbBr₃ NRs-ABS film before and after immersion in water for 138 days.

Video S1: Boiling water test of CsPbBr₃ NRs-PS composites. The CsPbBr₃ NRs-PS composite was put into boiling water and last for about 30 s (during which UV irradiation was also conducted), and then taken out to see brightness under UV irradiation.

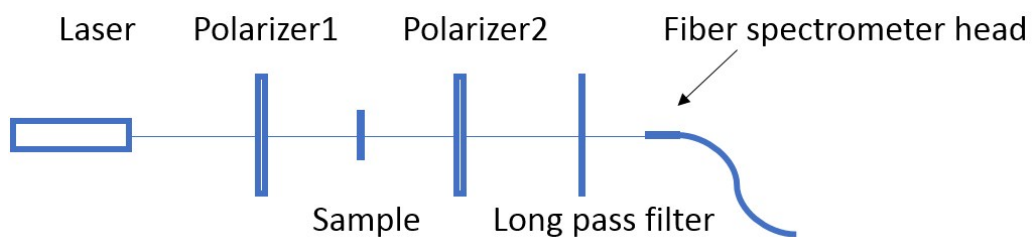


Figure S15. Polarization measurement setup for CsPbBr₃ NRs-PS samples. In each measurement polarizer 1 is fixed at certain angle while polarizer 2 is rotated stepwise from 0 – 360° and the spectrum at each angle is recorded.

To avoid error from the measurement setup, the sample is rotated for a certain angle and the angular dependence shifts accordingly, confirming that the polarization measured is sample-originated.

Table S3. Polarization level of the stretch-aligned NRs-PS synthesized at different conditions.

Spin speed	Polarization level			
	12 mg/mL	15 mg/mL	20 mg/mL	30 mg/mL
1k	0.20	0.14	0.14	0.15
2k	0.23	0.20	0.21	0.13
3k	0.14	0.19	0.16	0.13

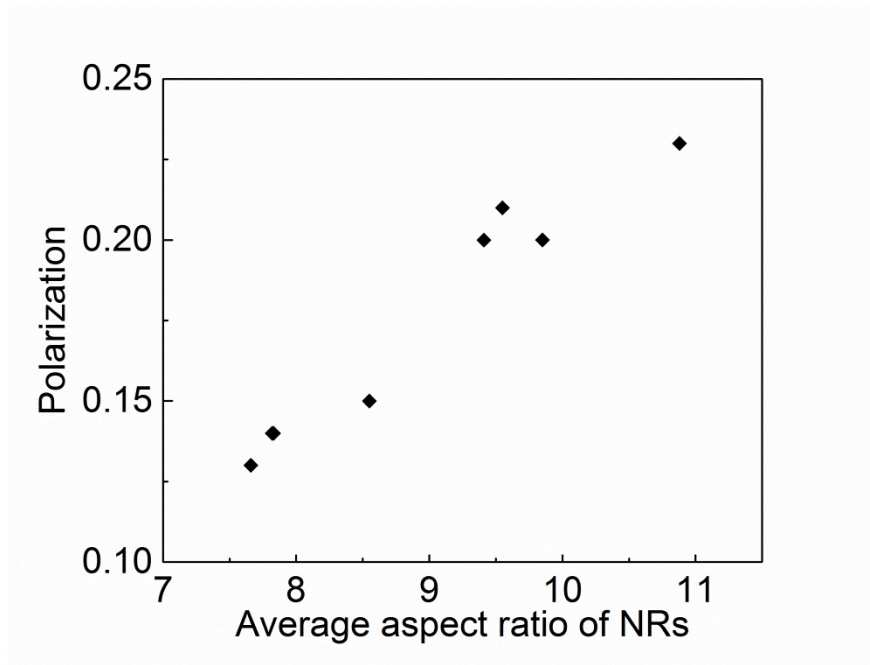


Figure S16. Correlation between polarization level of aligned NRs and NRs' average aspect ratio for CsPbBr₃ NRs-PS synthesized at 1000 rpm /2000 rpm spin speed with different precursor concentrations.

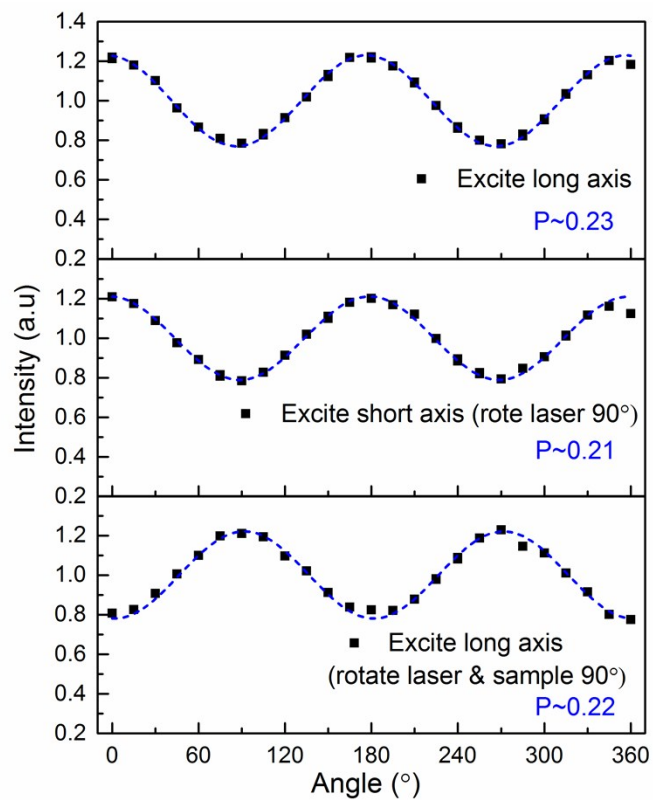


Figure S17. Emission polarization of stretch-aligned CsPbBr₃ NRs-PS when the excitation polarization is along long axis (up), short axis (middle) and long axis (both excitation and sample are rotated for 90° , down).

References:

1. Tenery, D.; Worden, J. G.; Hu, Z. J.; Gesquiere, A. J. *J. Lumin.* **2009**, *129*, 423-429.
2. Wang, J.; Gudiksen, M. S.; Duan, X.; Cui, Y.; Lieber, C. M. *Science* **2001**, *293*, 1455-1457.
3. Eaton, S. W.; Lai, M.; Gibson, N. A.; Wong, A. B.; Dou, L.; Ma, J.; Wang, L. W.; Leone, S. R.; Yang, P. *Proc. Natl. Acad. Sci.* **2016**, *113*, 1993-1998.